ORIGINAL ARTICLE

Cancer Science WILEY

BACH2-mediated FOS confers cytarabine resistance via stromal microenvironment alterations in pediatric ALL

Han Zhang[1] 🆔 | Ruidong Zhang[2] | Xueling Zheng[2] | Ming Sun[1] | Jia Fan[2] | Chunlian Fang[3] | Xin Tian[3] | Huyong Zheng[2]

[1]Institute of Medical Biology, Chinese Academy of Medical Sciences and Peking Union Medical College, Kunming, China

[2]Beijing Key Laboratory of Pediatric Hematology Oncology, National Key Discipline of Pediatrics (Capital Medical University), Key Laboratory of Major Diseases in Children, Ministry of Education, Hematology Oncology Center, Beijing Children's Hospital, National Center for Children's Health, Capital Medical University, Beijing, China

[3]Department of Hematology and Oncology, Kunming Children's Hospital (Children's Hospital of Kunming Medical University, Yunnan Children's Medical Center), Kunming, China

Correspondence
Han Zhang, Institute of Medical Biology, Chinese Academy of Medical Sciences and Peking Union Medical College, 935 Jiaoling Road, Kunming, Yunnan, 650118, China.
Email: jennifer_z@imbcams.com.cn

Funding information
National Natural Science Foundation of China, Grant/Award Number: 81900169; Fundamental Research Funds for the Central Universities, Grant/Award Number: 3332018130; Natural Science Foundation of Yunnan Province, Grant/Award Number: 2019FB089

Abstract

Acute lymphoblastic leukemia (ALL) is an aggressive hematological cancer that mainly affects children. Relapse and chemoresistance result in treatment failure, underlining the need for improved therapies. BTB and CNC homology 2 (BACH2) is a lymphoid-specific transcription repressor recognized as a tumor suppressor in lymphomas, but little is known about its function and regulatory network in pediatric ALL (p-ALL). Herein, we found aberrant BACH2 expression at new diagnosis not only facilitated risk stratification of p-ALL but also served as a sensitive predictor of early treatment response and clinical outcome. Silencing BACH2 in ALL cells increased cell proliferation and accelerated cell cycle progression. BACH2 blockade also promoted cell adhesion to bone marrow stromal cells and conferred cytarabine (Ara-C)–resistant properties to leukemia cells by altering stromal microenvironment. Strikingly, we identified *FOS*, a transcriptional activator competing with BACH2, as a novel downstream target repressed by BACH2. Blocking FOS by chemical compounds enhanced the effect of Ara-C treatment in both primary p-ALL cells and pre-B-ALL–driven leukemia xenografts and prolonged the survival of tumor-bearing mice. These data highlight an interconnected network of BACH2-FOS, disruption of which could render current chemotherapies more effective and offer a promising therapeutic strategy to overcome Ara-C resistance in p-ALL.

KEYWORDS

acute lymphoblastic leukemia, BACH2, bone marrow microenvironment, childhood, cytarabine

1 | INTRODUCTION

BACH2 is a lymphoid-specific transcription repressor encoded by the *BACH2* gene. BACH2 is expressed abundantly in B cells and plays critical roles in the development and differentiation of lymphocytes.[1-3] In common lymphoid progenitors, BACH2 promotes B cell development by repressing the myeloid program.[4] In pre-B cells, BACH2 is vital in negative selection at the pre-B cell receptor checkpoint.[5] At later stages, BACH2 and B cell lymphoma 6 (BCL6) cooperatively regulate germinal center B cell development, thus enabling immunoglobulin class-switch recombination and the somatic hypermutation of immunoglobulin genes.[1,2,6]

Han Zhang and Ruidong Zhang equally contributed to this work.

In addition to B cell development, large genome-wide association studies have identified numerous single-nucleotide variants in the human *BACH2* locus that are linked to multiple autoimmune and allergic diseases.[6] The mechanism underlying susceptibility to diverse immune-mediated diseases unveils additional roles of BACH2 in CD4^{+} T cell differentiation[7] and in maintaining the naïve state of T cells by suppressing effector memory T cell–related genes.[8] Given its essential roles in the development of B and T lymphocytes, BACH2 becomes more attractive to scientists in terms of its function in hematological malignancies.

Over the past decade, BACH2 has been gradually recognized as a tumor suppressor in some hematological neoplasms. For example, elevated levels of BACH2 in patients with diffuse large B cell lymphoma predict favorable outcomes.[9] Enforced expression of BACH2 in Burkitt's lymphoma cell line RAJI remarkably inhibits cell proliferation and sensitizes cells to chemotherapy drugs.[10] In mantle cell lymphoma, reduced BACH2 is associated with poor outcome in patients and chemoresistance in cell lines.[11] BACH2 has also been reported as a safeguard against leukemogenesis in leukemia.[5,12] One major mechanism of BACH2 downregulation in blood cancers is the loss of the long arm of chromosome 6 (6q) or the genetic lesions of its upstream activator paired box 5.[5,12,13] Despite its tumor suppressor–like roles in lymphomas, the function and downstream signaling of BACH2 in pediatric acute lymphoblastic leukemia (p-ALL) have so far remained elusive.

Pediatric ALL accounts for ~75% of pediatric leukemia, which is the most common cancer and one of the primary causes of death in children. In the past two decades, the overall survival rate of p-ALL has exceeded 90% in some developed countries,[14,15] even though treatment failure or relapsed events still occur in 15 ~ 20% of children with ALL.[16] Two major obstacles include incomplete understanding of leukemogenesis and lack of effective molecular targets in p-ALL.[14]

In the present study, we found BACH2 levels serve as a predictive factor for clinical outcome and chemoresistance in p-ALL patients on the basis of nearly 450 published p-ALL microarray data, and we tested this in an independent cohort of p-ALL samples. Further studies of BACH2 in ALL cell lines and primary cells revealed a tumor suppressor role of BACH2. Notably, we identified *FOS* as a downstream target of BACH2 in pre-B ALL cells. The interaction between BACH2 and FOS further enhanced cell adhesion to bone marrow (BM) and promoted Ara-C resistance by altering microenvironmental conditions. Blocking FOS activity by two chemicals significantly improved the efficiency of Ara-C treatment, both in vitro and in vivo. Our study lays the groundwork for future study on the signaling network of BACH2 in the pathogenesis and chemoresistance of p-ALL.

2 | MATERIALS AND METHODS

2.1 | Microarray data analysis

Microarray data from 284 children with p-ALL at new diagnosis (ND) and four BM samples from four healthy donors,[17] 35 ND relapse (RE)-matched pairs and 43 RE samples of p-ALL,[18] as well as 173 p-ALL samples at ND[19] were downloaded from the GEO database (http://www.ncbi.nlm.nih.gov/geo/; GSE28497, GSE3912, and GSE635, respectively). Microarray data from 20 leukemia cell lines[20] were downloaded from the Oncomine database (https://www.oncomine.org), an online microarray database. All above datasets are based on the same microarray platform of Human Genome U133A Array (Affymetrix). The log2 of mRNA expression values for *BACH2* and *FOS* in each dataset were used for analysis.

2.2 | Patients

Bone marrow (n = 11) and peripheral blood (n = 1) aspirates were obtained from children with ALL at ND approved by the Institutional Review Boards, with informed consent obtained from their parents or guardians in accordance with the Declaration of Helsinki. Patient characteristics are described in Table S1.

2.3 | Cell culture

Leukemic cells and BM stromal cells (BMSCs) were cultured in RPMI1640 and DMEM medium, respectively, supplemented with 10% FBS and 100 IU/mL penicillin-streptomycin. Cells were maintained under 5% CO_2 at 37°C.

2.4 | RNA isolation and real-time RT-PCR

RNA was isolated as previously described,[11] followed by real-time RT-PCR using a One Step SYBR PrimeScript PLUS RT-PCR kit (Takara). The relative expression level of each gene was normalized to the *GAPDH* by the method of $2^{-\Delta\Delta Ct}$.

2.5 | Lentivirus generation and infection

293T cells were transfected with either lentiviral shRNAs specific for human BACH2 (GE Dharmacon, clone ID: V3LHS_363286 and V3LHS_409004) or a nonsilencing lentiviral shRNA control plasmid (GE Dharmacon) or the open reading frame (ORF) of human BACH2 (GE Dharmacon, clone ID: PLOHS_100066339). Lentiviruses were collected 48 hours post transfection. Cells were then infected with lentiviruses using polybrene (8 μg/mL). Lentiviral-transduced cells were selected with puromycin (2 μg/mL) or blasticidin (5 μg/mL) for 14 days.

2.6 | Immunoblotting assay and semiquantitative analysis

Harvested cells were lysed to perform immunoblotting assay as previously described.[21] The antibodies were used for

immunoblots: anti-BACH2, anti-FOS, and anti-GAPDH (Cell Signaling). Immunoblotting was subjected to semiquantitative analysis using an ImageJ software. The relative expression of target proteins was normalized to GAPDH.

2.7 | Cell viability assay and IC$_{50}$

Leukemic cells were treated with Ara-C for 48 hours, and cytotoxicity was assessed with fluorometric method using CellTiter-Blue® (Promega).[21] The Hill-slope logistic model was used to calculate IC$_{50}$ values using a CompuSyn software (ComboSyn).

2.8 | Cell cycle analysis and intracellular BrdU incorporation assay

Cell cycle and intracellular BrdU incorporation were performed using PI/RNase Staining Buffer and an APC BrdU Flow kit (BD Biosciences), respectively, as previously described.[11] Staining cells were analyzed on a NovoCyte flow cytometer (ACEA Biosciences) or CytoFLEX flow cytometer (Beckman Coulter). The data were further analyzed using a FlowJo software.

2.9 | Cell proliferation and apoptosis assays

PKH26 dye (Sigma-Aldrich) and PE Annexin V Apoptosis Detection kit (BD Biosciences) were used to detect cell proliferation and apoptosis.[11]

2.10 | Cell adhesion assay

Cell adhesion was performed as previously described.[21] PKH26 dye intensity was measured using FlexStation3 (Molecular Devices). Representative pictures were taken using a Leika DMIL LED Fluorescence microscope (Leica). For neutralization experiments, human GM-CSF antibodies (1 µg/mL), IL-8 antibodies (1 µg/mL), IL-6 antibodies (0.5 µg/mL), or IgG1 isotype control antibodies were used (R&D systems).

2.11 | Cytokines analysis

Leukemic cells were plated onto the pre-established monolayer of HS-5 cells and allowed to coculture for 48 hours in 5% CO_2 at 37°C (complete RPMI1640: complete DMEM = 1:1). Coculture media were collected and measured by a multiplexed flow cytometric assay using a human cytokine kit (HCYTOMAG-60K-08) on a Luminex® system (MAGPIX® with xPONENT). Eight cytokines including G-CSF, GM-CSF, MIP-1α, IL-1α, IL-1β, IL-1ra, IL-6, and IL-8 were detected (MILLIPLEX® Analyst 5.1). Samples were measured in duplicates with the coefficient of variation (CV) <20%. Human GM-CSF (4A Biotech), IL-6, and IL-8 (NeoBioscience) were determined respectively by ELISA assays.

2.12 | Luciferase activity assay

Luciferase activity was measured using a Dual-Luciferase Reporter Assay System kit (Promega).[11] The data were normalized and presented as the ratio of firefly/*Renilla* luciferase activities.

2.13 | Cleavage under targets and tagmentation (CUT&Tag) sequencing

CUT&Tag libraries were generated using Nalm-6 cells, followed by sequencing on an Illumina NovaSeq 6000 sequencer (Biomarker Technologies). Integrative Genomics Viewer (IGV v2.8.3) software[22] was used to perform peak analysis using GRCh38 as a human genome reference. The detailed procedures are indicated in Supplementary methods.

2.14 | Tumor xenograft model

BALB/C nude mice (5 weeks old) were purchased from Charles River Laboratories and housed in the barrier conditions at the Institute of Medical Biology (IMB). All animal procedures were approved by the IMB Animal Care Committee. All mice were pretreated with an intraperitoneal (ip) injection of CTX at a dose of 100 mg/kg once daily for two consecutive days. Mice were then injected intravenously (iv) with manipulated Nalm-6 cells via tail vein (5×10^6 cells/mouse) to perform further analysis.

2.15 | Statistical analysis

Data are described as experimental mean $\pm$ standard error of mean (SEM) or standard deviation (SD). Statistical significance of differences between control and experimental groups was evaluated by the Student t test, where $*P < .05$, $**P < .01$, and $***P < .001$ are considered statistically significant. All experiments and assays were repeated at least twice and performed in duplicate or triplicate.

3 | RESULTS

3.1 | Expression feature of *BACH2* is associated with risk stratification and early treatment responses

To determine the clinical relevance of BACH2 in p-ALL, we firstly analyzed the expression values of *BACH2* based on one published microarray data (GSE28497) from 284 children with ALL at ND.

Compared with normal BM CD19$^+$CD10$^+$ cells from four healthy donors, leukemic cells from p-ALL samples showed reduced *BACH2* levels (Figure 1A). Interestingly, we found lower *BACH2* levels in patients with T cell ALL (T-ALL), who have poorer outcomes, than in patients with B cell ALL (B-ALL)[23] (Figure 1B). Among B-ALL samples, patients with unfavorable *BCR-ABL1* fusion gene had remarkably lower *BACH2* levels than patients without *BCR-ABL1* (Figure 1C). In contrast, *BACH2* expression in patients who had a favorable genetic subtype (*ETV6-RUNX1*$^+$) or low-to-intermediate risk subtype (*TCF3-PBX1*$^+$) of B-ALL was higher compared with patients who did not (Figure 1D-E and Figure S1A), suggesting that differential expression of *BACH2* could facilitate risk classification of p-ALL.

Given that minimal residual disease (MRD) tracking plays a crucial role in early outcome prediction for p-ALL, we next analyzed the correlation between *BACH2* expression and MRD response. As shown in Figure 1F, patients with lower *BACH2* levels at ND were more inclined to occur MRD positive (MRD$^+$) at day 19 (d19) from diagnosis, and this tendency became more significant at d46 (Figure 1G). Intriguingly, MRD$^+$ at d19 turned into MRD negative (MRD$^-$) at d46 in patients with higher *BACH2* levels in B-ALL compared with those with lower *BACH2* levels, and the same is true in T-ALL (Figure S1B-C). Strikingly, *BACH2* levels in different subtypes at ND also coincided with the MRD monitoring at d19 or d46. For example, the highest *BACH2* levels were observed in patients with *TCF3-PBX1* (Figure 1E), while the smallest proportion of MRD$^+$ patients were found at either d19 or d46 (Figure S1D). These data suggest that aberrant expression of *BACH2* at ND is very likely to be a predictor of the early treatment response during induction phase.

In addition to ND samples, further analysis from another microarray dataset (GSE3912) revealed that early MRD response is also predictive of the degree of *BACH2* expression at RE: The higher percentages of MRD at d36, the lower levels of *BACH2* at RE (Figure 1H), and a much stronger inverse correlation between %MRD and *BACH2* expression was observed in T-ALL (Figure S1E), suggesting a reciprocal dependency of *BACH2* and MRD on their respective role in outcome prediction.

3.2 | BACH2 is a sensitive predictor of clinical outcome in p-ALL

To validate the above microarray analysis, we examined the mRNA and protein levels of BACH2 in an independent cohort of p-ALL samples at ND (n = 12). Indeed, *BACH2* levels were significantly lower in p-ALL samples compared with CD19$^+$ cells from patients with immune thrombocytopenic purpura (ITP), a nontumorous hematologic disorder of megakaryocyte without disturbing lymphocytes (Figure 2A). Of note, in addition to a patient with T-ALL, there was one patient with B/T cell mixed-phenotype acute leukemia (B/T MPAL), a high-risk subtype of ALL with a uniformly poor outcome.[24] *BACH2* levels were much lower in T-ALL and B/T MPAL cases compared with B-ALL cases (Figure 2B), and the lowest expression of

BACH2 was observed in a B/T MPAL patient (Figure 2C). Interestingly, among B-ALL cases, there is one special case (Pt #12) that showed the lowest levels of *BACH2* compared with others (Figure 2D). When reviewing the clinical information for this patient, we discovered that she had a very high tumor burden in peripheral blood at ND (90% of blasts), and passed away soon after induction therapy (Table S1). This, together with a close relationship between *BACH2* and MRD as indicated above, further supported the possibility that BACH2 may serve as a sensitive predictor of risk classification and clinical outcome, although additional evidence from more clinical samples is needed.

Similarly, immunoblots of BACH2 showed that patients with a favorable subtype (*ETV6-RUNX1*$^+$) exhibited higher expression of BACH2 compared with patients with unfavorable subtypes (*BCR-ABL1*$^+$, B/T MPAL, and T-ALL; Figure 2E), in agreement with both the microarray analysis and the mRNA findings.

3.3 | Knockdown of BACH2 accelerates cell proliferation in vitro and increases leukemia burden in vivo

To better delineate the biological roles of BACH2 in leukemic cells, we silenced BACH2 (BACH2^{KD}) in two human ALL cell lines, Nalm-6 and Reh. The knockdown efficiency of BACH2 in leukemic cells was evaluated by immunoblots which showed a better knockdown efficiency of BACH2^{KD}-2 than BACH2^{KD}-1 in both cell lines; meanwhile, we generated stable BACH2-overexpressing (BACH2^{OE}) Nalm-6 and Reh cells (Figure 3A). Compared with control cells (BACH2^{Con}), BACH2 silencing significantly increased cell growth, whereas BACH2-overexpressing cells showed lower growth rates in both cell lines (Figure 3B), indicating a potential antitumor role of BACH2 in leukemic cells. Due to a better knockdown efficiency and a significant cell growth phenotype of BACH2^{KD}-2 cells, BACH2^{KD}-2 was selected to perform the subsequent experiments.

To elucidate the mechanism involving enhanced cell growth upon BACH2 silencing, cell proliferation was analyzed by staining cells with PKH26 dye to track cell division. PKH26 fluorescent labeling was declined rapidly in both cell lines upon BACH2 silencing, while BACH2-overexpressing cells showed a slow decline in PKH26 labeling compared with control cells, indicating that downregulation of BACH2 promotes cell proliferation (Figure 3C). Further analysis of cell cycle distribution in manipulated Nalm-6 and Reh cells showed approximately 10% more cells in S phase upon BACH2 silencing compared with control cells, whereas the diminished proliferation in BACH2-overexpressing cells was associated with decreased S-G2/M population (Figure 3D and Figure S2A). Intracellular pulse staining for BrdU incorporation further confirmed higher amounts of cells in S phase after BACH2 silencing but lower amounts of S phase cells upon BACH2 overexpression in both cell lines (Figure 3E and Figure S2B). These data indicated that silencing BACH2 leads to increased cell proliferation and accelerated cell cycling, thus contributing to a dominant growth.
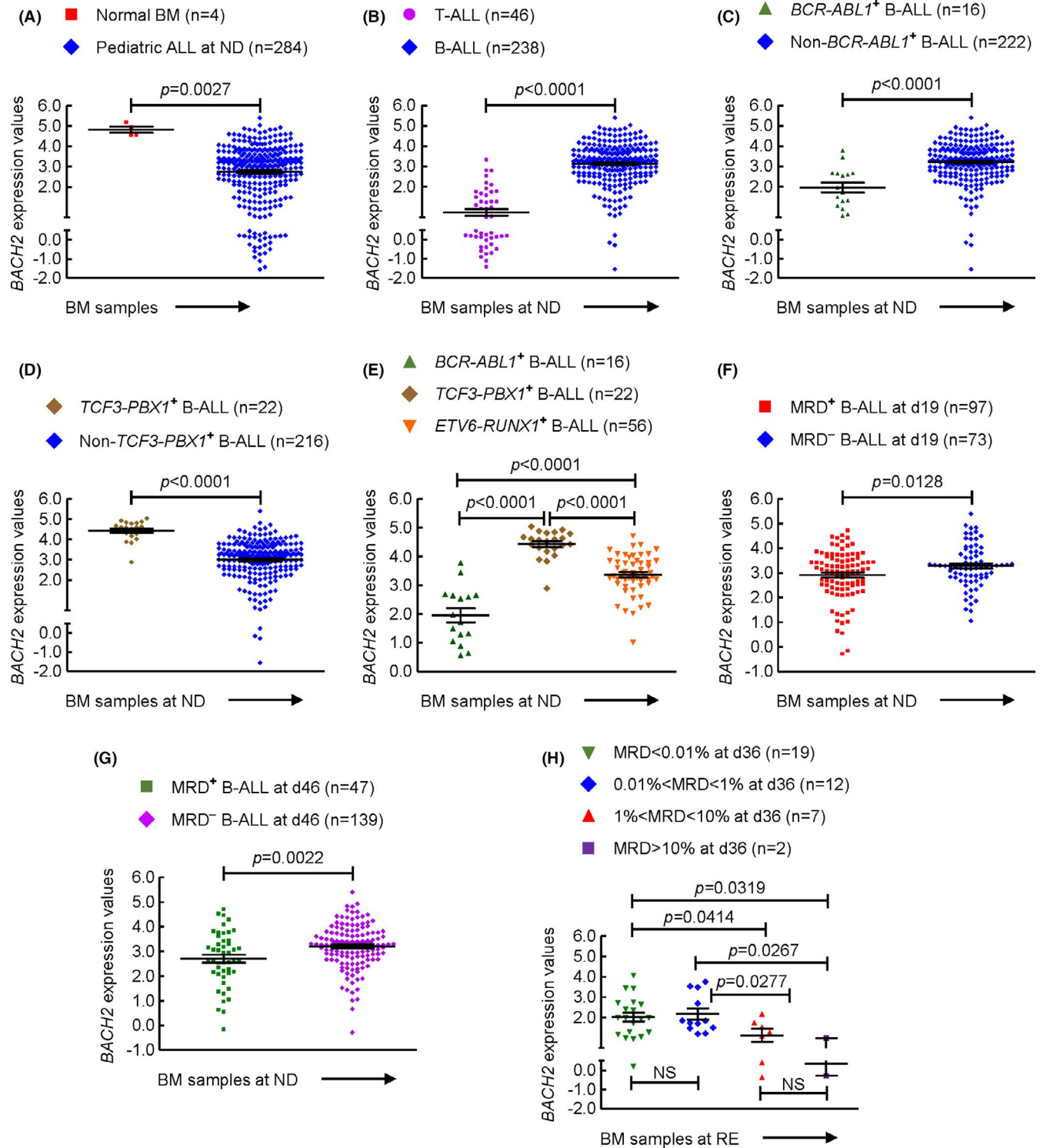
FIGURE 1 Expression feature of *BACH2* levels in pediatric acute lymphoblastic leukemia (p-ALL) from microarray data. A, *BACH2* mRNA levels were downregulated in bone marrow (BM) cells from p-ALL at new diagnosis (ND) (n = 284) compared with CD19⁺CD10⁺ BM cells from healthy donors (n = 4). B, BM cells from T cell ALL (T-ALL) (n = 46) contained lower levels of *BACH2* than BM cells from B cell ALL (B-ALL) at ND (n = 238). C, BM cells from B-ALL with *BCR-ABL1* fusion gene at ND (n = 16) contained lower levels of *BACH2* compared with those from B-ALL without *BCR-ABL1* fusion gene (n = 222). D, BM cells from *TCF3-PBX1*⁺ B-ALL at ND (n = 22) contained higher *BACH2* levels than those from B-ALL without *TCF3-PBX1* fusion gene (n = 216). E, Comparison of *BACH2* levels in BM among different subtypes. B-ALL patients with lower *BACH2* levels in BM became minimal residual disease positive (MRD⁺) at d19 from diagnosis (F) and remained MRD⁺ at day 46 (G). H, Inverse correlation between %MRD and *BACH2* levels in BM from relapse (RE) samples at d36 (M1 patients). Data are shown as the mean ± SEM
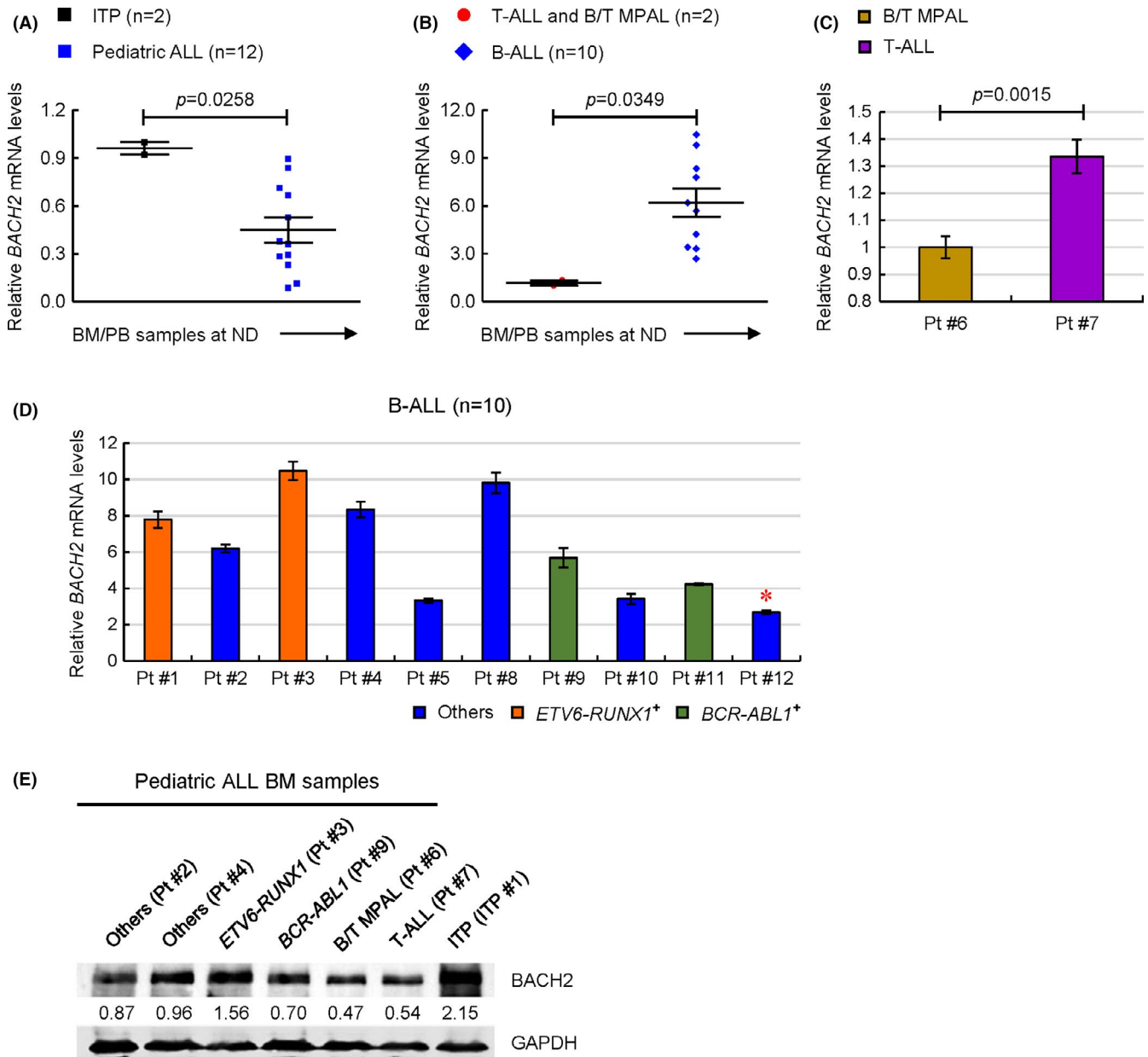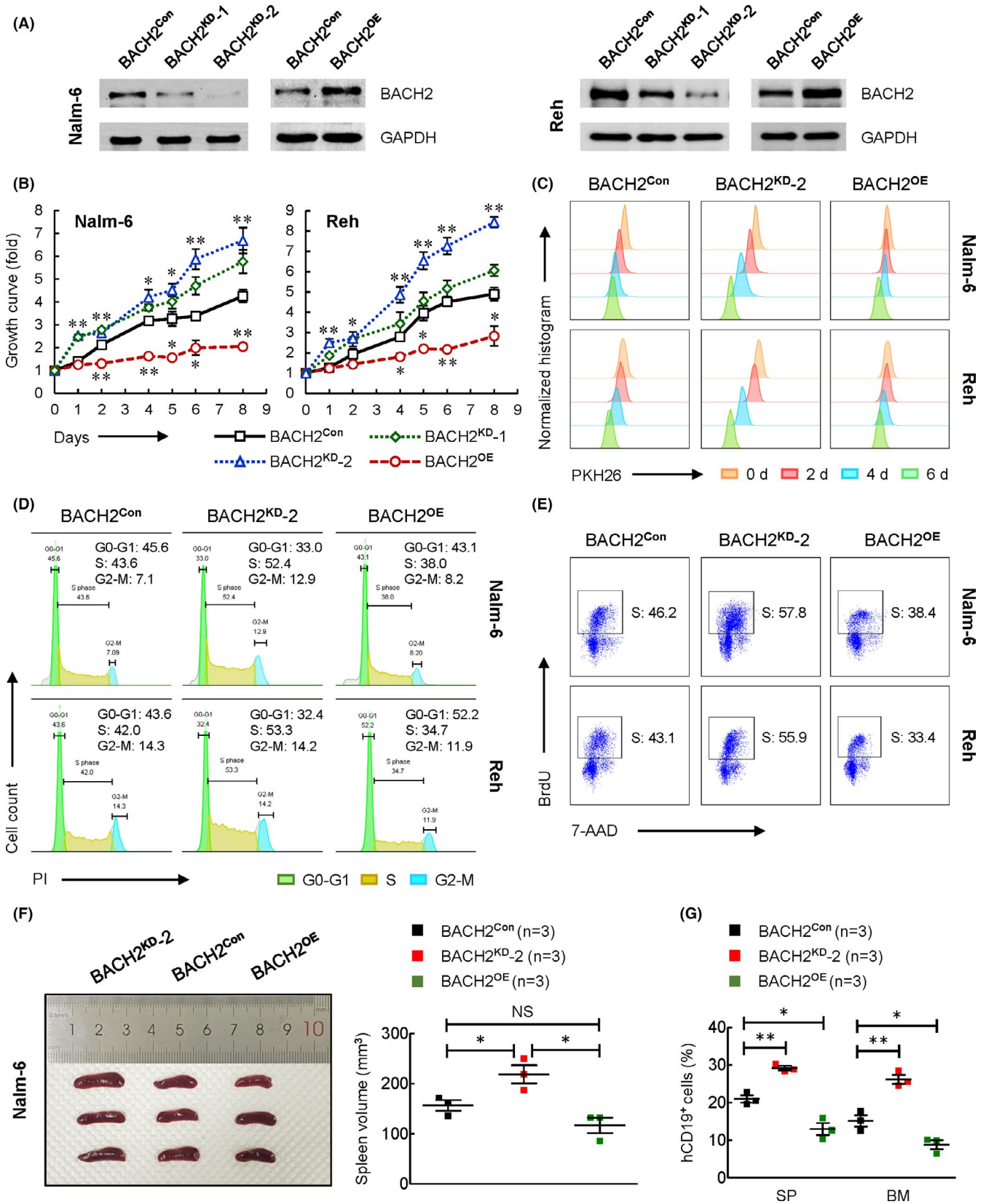
FIGURE 2 Decreased BACH2 levels are associated with clinical outcome in pediatric acute lymphoblastic leukemia (p-ALL). A, *BACH2* mRNA levels were lower in p-ALL samples at new diagnosis (ND) (n = 12) compared with samples from patients with immune thrombocytopenic purpura (ITP) (n = 2). Each condition was run in triplicate with the values normalized to *GAPDH*. Data are shown as the mean ± SEM. B, Leukemic cells in T cell ALL (T-ALL) and B/T cell mixed-phenotype acute leukemia (B/T MPAL) (n = 2) contained lower levels of *BACH2* than those in B cell ALL (B-ALL) (n = 10). Data are shown as the mean ± SEM. C, *BACH2* levels in T-ALL and B/T MPAL. D, *BACH2* levels in B-ALL. The red asterisk indicates patient #12 (Pt #12) with the lowest levels of *BACH2*. E, Immunoblots of BACH2 in different subtypes of p-ALL with one ITP sample as a negative control. GAPDH was used as a loading control. BM, bone marrow

FIGURE 3 Silencing BACH2 increases cell proliferation and accelerates cell cycle progression. A, The knockdown and overexpressed efficiency of BACH2 (BACH2^{KD} and BACH2^{OE}) in Nalm-6 (left) and Reh (right) cells were validated using immunoblots respectively with a nonsilencing shRNA plasmid (BACH2^{Con}) as a negative control. GAPDH was used as a loading control. B, Viable cells were counted in manipulated Nalm-6 and Reh cells. C, Manipulated acute lymphoblastic leukemia (ALL) cells were stained with PKH26 fluorescent dye which was analyzed using flow cytometry (FCM). Representative FCM analyses at 0, 2, 4, and 6 are shown. D, Representative cell-cycle distribution of manipulated Nalm-6 and Reh cells. E, Representative intracellular pulse staining of BrdU in manipulated Nalm-6 and Reh cells. F, BACH2^{KD}-2, BACH2^{OE}, or BACH2^{Con} Nalm-6 cells were intravenously injected into mice (n = 3). Xenografts were humanely sacrificed 7 d post transplantation, and the spleens (SPs) were isolated and photographed against a ruler (left). The sizes of the SPs in each group were measured (right). Data are shown as the mean ± SEM. NS, not significant; *P < .05 (vs control group). G, Human CD19^{+} (hCD19^{+}) cells were isolated from SP and bone marrow (BM) using anti-hCD19-MicroBeads, and the % of hCD19^{+} cells in each organ was calculated. Data are presented as the mean ± SEM. *P < .05; **P < .01 (vs control xenografts)

(A)

Nalm-6: BACH2^{Con}, BACH2^{KD}-1, BACH2^{KD}-2, BACH2^{Con}, BACH2^{OE} — BACH2, GAPDH

Reh: BACH2^{Con}, BACH2^{KD}-1, BACH2^{KD}-2, BACH2^{Con}, BACH2^{OE} — BACH2, GAPDH

(B) Growth curve (fold) vs Days — Nalm-6 and Reh

BACH2^{Con} — BACH2^{KD}-1 — BACH2^{KD}-2 — BACH2^{OE}

(C) Normalized histogram, PKH26 — BACH2^{Con}, BACH2^{KD}-2, BACH2^{OE} (Nalm-6, Reh)
0 d — 2 d — 4 d — 6 d

(D) Cell count, PI — BACH2^{Con}, BACH2^{KD}-2, BACH2^{OE}

Nalm-6:
BACH2^{Con}: G0-G1: 45.6, S: 43.6, G2-M: 7.1
BACH2^{KD}-2: G0-G1: 33.0, S: 52.4, G2-M: 12.9
BACH2^{OE}: G0-G1: 43.1, S: 38.0, G2-M: 8.2

Reh:
BACH2^{Con}: G0-G1: 43.6, S: 42.0, G2-M: 14.3
BACH2^{KD}-2: G0-G1: 32.4, S: 53.3, G2-M: 14.2
BACH2^{OE}: G0-G1: 52.2, S: 34.7, G2-M: 11.9

G0-G1 — S — G2-M

(E) BrdU vs 7-AAD — BACH2^{Con}, BACH2^{KD}-2, BACH2^{OE}
Nalm-6: S: 46.2, S: 57.8, S: 38.4
Reh: S: 43.1, S: 55.9, S: 33.4

(F) Nalm-6: BACH2^{KD}-2, BACH2^{Con}, BACH2^{OE}

Spleen volume (mm^3): BACH2^{Con} (n=3), BACH2^{KD}-2 (n=3), BACH2^{OE} (n=3)
NS, *, *

(G) hCD19$^+$ cells (%) — SP, BM
BACH2^{Con} (n=3), BACH2^{KD}-2 (n=3), BACH2^{OE} (n=3)
**, *, **, *

To demonstrate in vivo relevance, we intravenously transplanted manipulated Nalm-6 cells into mice (Figure S2C). BACH2^{KD} xenografts developed larger spleens (SPs) as compared with the BACH2^{OE} and control xenografts (Figure 3F). Further analysis or these xenografts displayed increased human CD19$^+$ (hCD19$^+$) cells in the SP and BM upon BACH2 silencing, indicating higher leukemia burden in BACH2^{KD} xenografts; by contrast, lower leukemia burden was observed in BACH2^{OE} xenografts (Figure 3G).
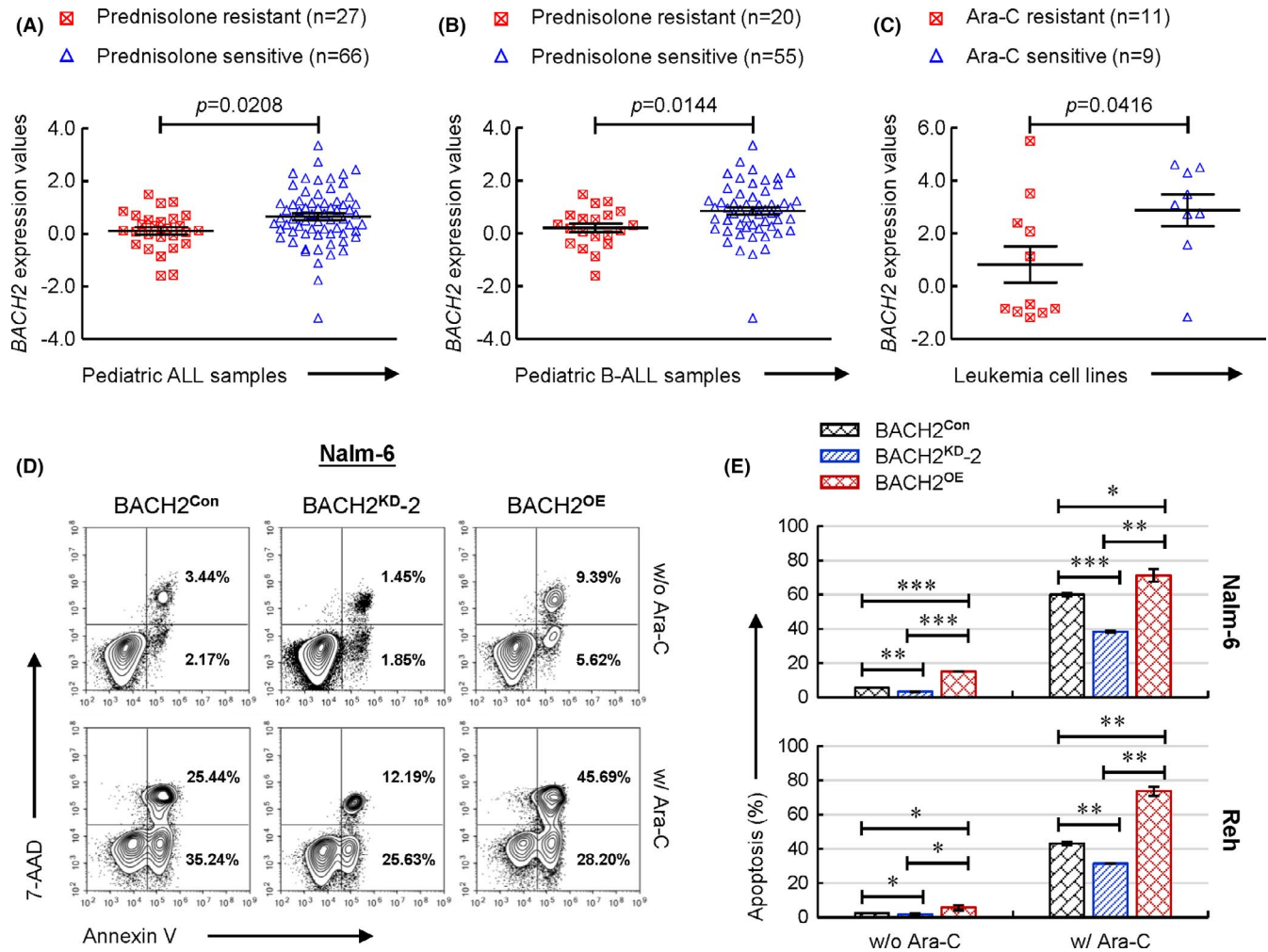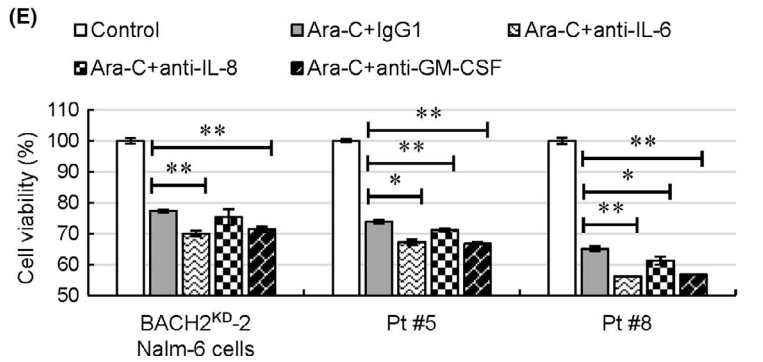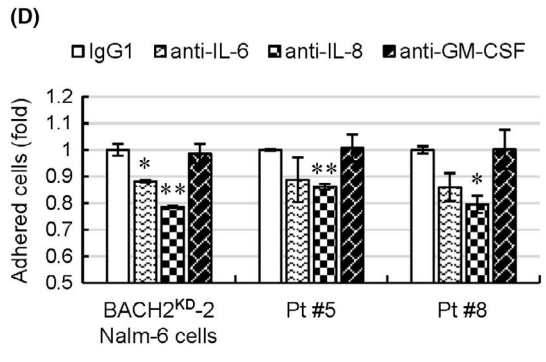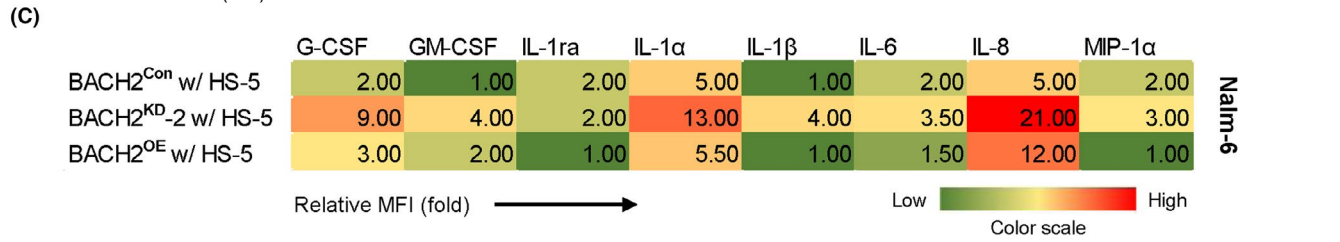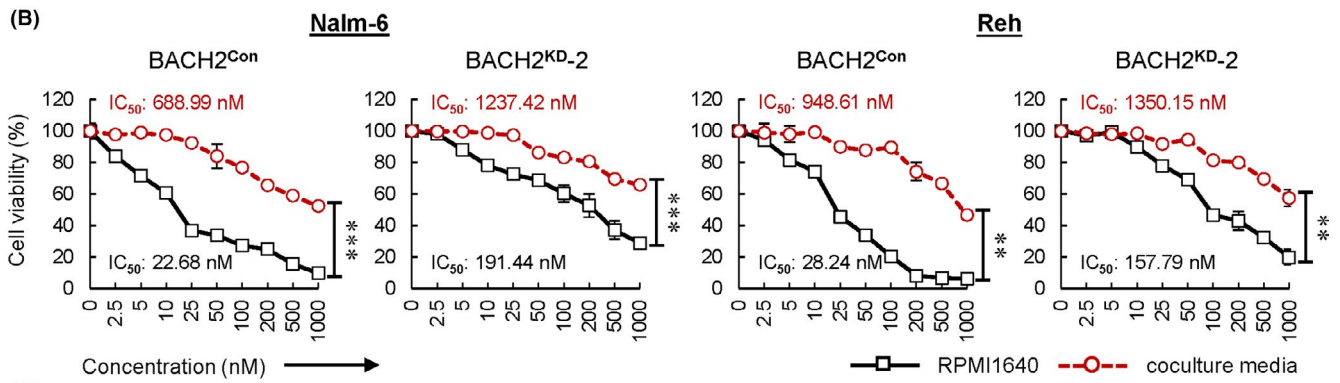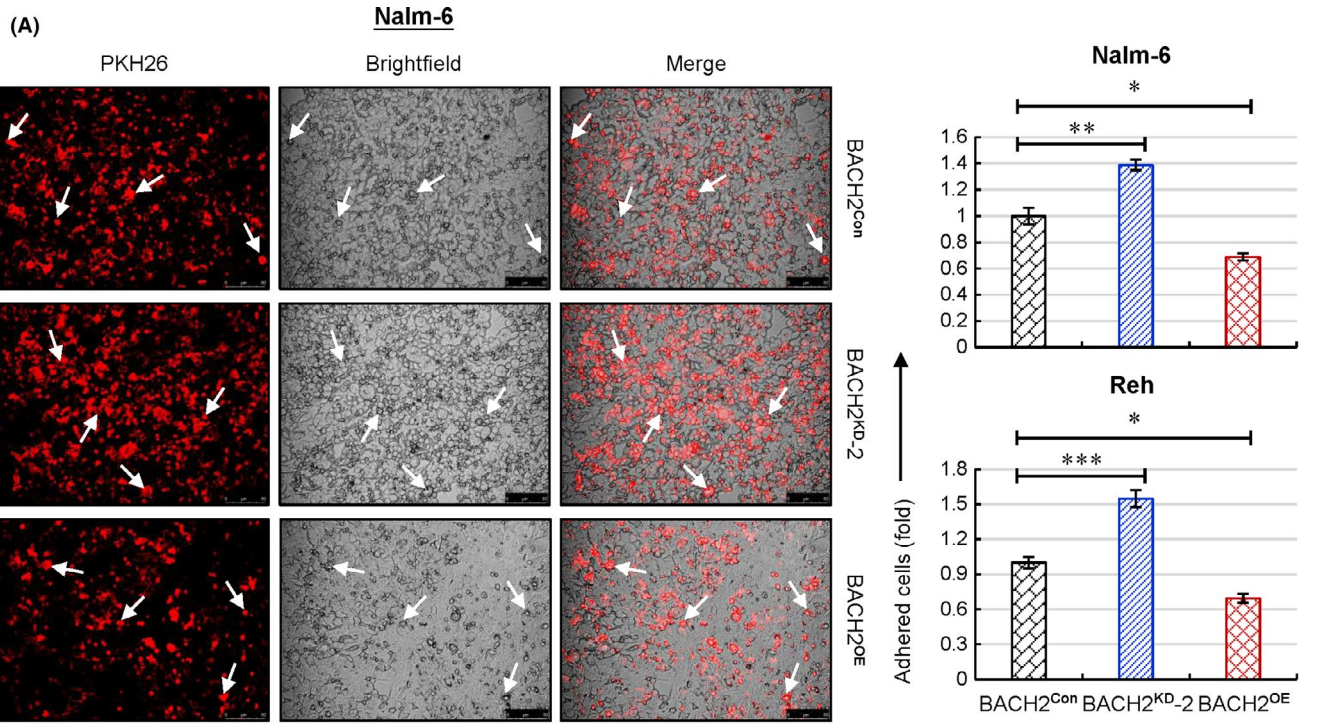
FIGURE 4 Decreased BACH2 expression confers chemo-resistant properties to pediatric acute lymphoblastic leukemia (p-ALL). A, Children with ALL from the prednisolone-resistant group (n = 27) had lower *BACH2* levels than those from the prednisolone-sensitive group (n = 66). B, Children with B cell ALL (B-ALL) in the prednisolone-resistant group (n = 20) had lower *BACH2* levels than those in the prednisolone-sensitive group (n = 55). C, Leukemia cell lines with lower *BACH2* expression (n = 11) were more resistant to Ara-C compared with those with higher *BACH2* levels (n = 9). Data are shown as the mean ± SEM. D, Manipulated Nalm-6 and Reh cells were treated with or without Ara-C treatment, and cell survival was detected by staining cells with Annexin V/7-AAD. Representative flow cytometry (FCM) analyses in Nalm-6 cells are shown. E, The % population of apoptotic cells in each group is shown as the mean ± SD from two independent experiments. *$P < .05$; **$P < .01$; ***$P < .001$ (vs control group). w/, with; w/o, without

FIGURE 5 BACH2 silencing promotes cell adhesion and Ara-C resistance by altering stromal microenvironment. A, Cells were stained with PKH26 prior to seeding onto a pre-established monolayer of HS-5 bone marrow stromal cells (BMSCs). Representative microscopic images of adherent manipulated Nalm-6 cells are shown in a coculture setting. Scale bar, 50 μm. The arrows point to the representative leukemic cells adhered to BMSCs (left). PKH26 dye intensity in manipulated Nalm-6 and Reh cells were normalized to the control cells. Data are shown as the mean ± SD from two independent experiments (right). B, Manipulated Nalm-6 and Reh cells were cultured in complete RPMI1640 media or coculture media upon treatment of Ara-C for 48 h. Cell viability was determined using MTT assays. IC$_{50}$ values of Ara-C for BACH2^{Con} or BACH2^{KD}-2 cells are indicated, with red representing cells in coculture media (upper) and black representing cells in complete RPMI1640 media (lower). C, Relative mean fluorescent intensity (MFI) of multiple cytokines in coculture media. The fold change in expression compared with the lowest value is indicated by the color intensity, with green representing reduced expression and red representing elevated expression. w/, with. D, Primary BM cells from two p-ALL patients (Pt #5 and Pt #8) or BACH2^{KD}-2 Nalm-6 cells were stained with PKH26 prior to seeding onto a pre-established monolayer of HS-5 BMSCs. PKH26-stained cells were allowed to adhere for 4 h with neutralizing antibodies of IL-6 (0.5 μg/mL), IL-8, or GM-CSF (1 μg/mL). IgG1 antibody (1 μg/mL) was used as a negative control. PKH26 dye intensity of leukemic cells was normalized to those without neutralizing antibodies in each group. E, Primary cells or BACH2^{KD}-2 Nalm-6 cells were treated with Ara-C (20 nmol/L) for 48 h with neutralizing antibodies of IL-6 (0.5 μg/mL), IL-8, or GM-CSF (1 μg/mL). IgG1 antibody (1 μg/mL) was used as a negative control. Cell viability was determined using MTT assays. Data are normalized to nontreated control cells and shown as the mean ± SD from three independent experiments. *$P < .05$; **$P < .01$; ***$P < .001$ (vs control group)

(A) Nalm-6

PKH26 | Brightfield | Merge

BACH2^Con, BACH2^KD-2, BACH2^OE

Nalm-6

Reh

Adhered cells (fold)

BACH2^Con BACH2^KD-2 BACH2^OE

(B) Nalm-6 / Reh

BACH2^Con: IC$_{50}$: 688.99 nM, IC$_{50}$: 22.68 nM
BACH2^KD-2: IC$_{50}$: 1237.42 nM, IC$_{50}$: 191.44 nM
BACH2^Con: IC$_{50}$: 948.61 nM, IC$_{50}$: 28.24 nM
BACH2^KD-2: IC$_{50}$: 1350.15 nM, IC$_{50}$: 157.79 nM

Cell viability (%) — Concentration (nM)

RPMI1640 — coculture media

(C)

	G-CSF	GM-CSF	IL-1ra	IL-1α	IL-1β	IL-6	IL-8	MIP-1α	
BACH2^Con w/ HS-5	2.00	1.00	2.00	5.00	1.00	2.00	5.00	2.00	Nalm-6
BACH2^KD-2 w/ HS-5	9.00	4.00	2.00	13.00	4.00	3.50	21.00	3.00	
BACH2^OE w/ HS-5	3.00	2.00	1.00	5.50	1.00	1.50	12.00	1.00	

Relative MFI (fold)

Low — High
Color scale

(D) ☐ IgG1 ☒ anti-IL-6 ☒ anti-IL-8 ◼ anti-GM-CSF

Adhered cells (fold)

BACH2^KD-2 Nalm-6 cells | Pt #5 | Pt #8

(E) ☐ Control ☒ Ara-C+IgG1 ☒ Ara-C+anti-IL-6
☒ Ara-C+anti-IL-8 ◼ Ara-C+anti-GM-CSF

Cell viability (%)

BACH2^KD-2 Nalm-6 cells | Pt #5 | Pt #8

3.4 | Decreased BACH2 expression confers chemoresistant properties to p-ALL

We next questioned the implication of reduced *BACH2* levels in p-ALL treatment. Based on published microarray data (GSE635) from 173 p-ALL cases at ND, patients with lower *BACH2* levels predisposed to prednisolone resistance (Figure 4A), and this tendency became more significant in the B-ALL group (Figure 4B). Leukemic cell lines (https://www.oncomine.org) with decreased *BACH2* expression were also likely to occur resistant to cytarabine (Ara-C; Figure 4C), one of the antimetabolites used to induce remission in ALL.[25,26] It is interesting to note that BACH2 promotes oxidative stress–induced cell death,[27] and Ara-C is a strong oxidative stressor that can induce the nuclear accumulation of BACH2 in lymphocytes,[10] suggesting a close correlation between Ara-C treatment and BACH2-mediated pathway. Thus, we used Ara-C as an agent to investigate the potential BACH2-mediated chemoresistant mechanisms.

To confirm whether BACH2 blockade contributes to Ara-C resistance in leukemic cells, we firstly revealed a survival advantage of the BACH2[KD] Nalm-6 cells compared with control cells, whereas a higher proportion of apoptotic cells were found in the BACH2[OE] Nalm-6 cells (Figure 4D-E), indicating that silencing BACH2 contributes to enhanced leukemic cell survival. After introducing Ara-C into Nalm-6 cells, BACH2 deletion displayed lower drug sensitivity by preventing cell apoptosis, which was reversed by BACH2 overexpression (Figure 4D-E), and similar results were observed in manipulated Reh cells (Figure 4E). Notably, further analysis revealed a striking increase in the proportion of late apoptotic cells upon BACH2 overexpression in both cell lines after Ara-C treatment compared with control and BACH2-silenced cells, suggesting that overexpression of BACH2 accelerates cell apoptosis from the early phase to the late phase (Figure S3). Collectively, these data demonstrated that BACH2 downregulation confers Ara-C resistance properties to leukemic cells by likely increasing the threshold for drug-induced apoptosis.
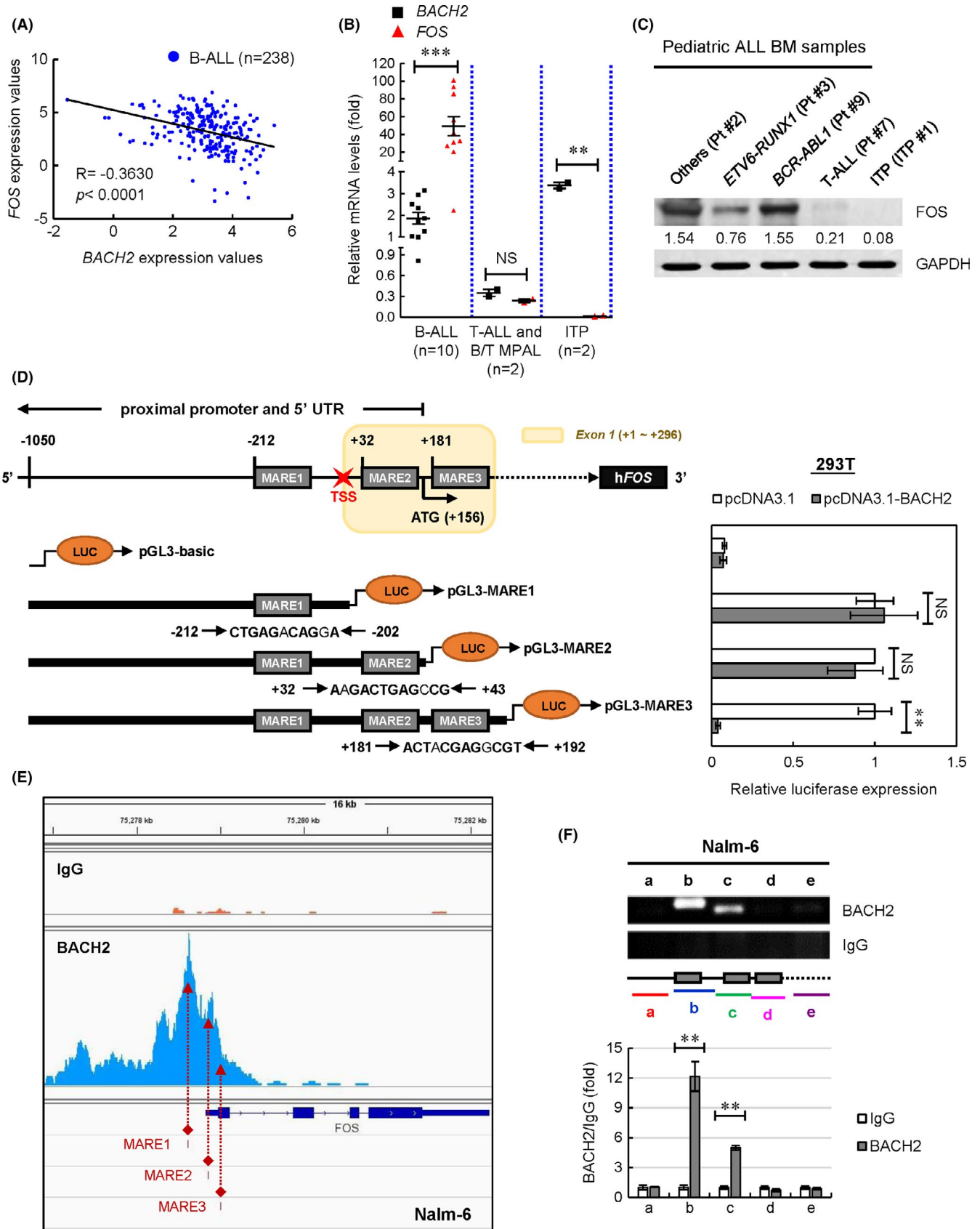
3.5 | BACH2 silencing promotes cell adhesion and Ara-C resistance by altering stromal microenvironment

BMSCs are regarded as a safeguard to protect BM-resident leukemic cells from chemotherapy-induced apoptosis by producing multiple growth factors and cytokines, leading to stroma-mediated chemoresistance.[28-31] Thus, BM microenvironmental remodeling has become a key parameter and prognostic factor in leukemia.[32] As BACH2[KD] xenografts showed increased leukemia burden to the BM (Figure 3F), we then used a coculture model of leukemic cells and BMSCs to investigate the effect of BACH2 on cell adhesion and complex leukemia-stroma network, and how such an effect modifies the cytotoxicity of Ara-C within the surrounding stroma.

Compared with control cells, silencing BACH2 in Nalm-6 and Reh cells resulted in a significant increase in cell adhesion to the HS-5 BMSCs, while decreased cell adhesion was observed upon BACH2 overexpression in both cell lines (Figure 5A). Interestingly, the coculture media showed protective effects against Ara-C with much higher IC$_{50}$ values, no matter whether in control or in BACH2[KD] cells (Figure 5B), suggesting that BMSCs-secreted cytokines are very likely involved in Ara-C resistance of BM-resident leukemic cells. Indeed, further analysis using coculture media revealed substantial changes in the secretion of many growth factors and cytokines that play pivotal roles in the maintenance of a normal BM microenvironment[33-35] (Figure 5C). Coculturing HS-5 with BACH2[KD] Nalm-6 cells resulted in significant upregulation of GM-CSF, IL-6, and IL-8 compared with control cells, whereas IL-6, IL-8, and MIP-1α were decreased when coculturing HS-5 with BACH2[OE] Nalm-6 cells (Figure S4A). These results were further validated by ELISA assays respectively for single cytokine from independent experiments (Figure S4B).

To extend our findings to primary cells, we performed experiments with BM cells from two p-ALL patients using a similar coculture setting. Primary cells or drug-resistant BACH2[KD] Nalm-6 cells did get great benefit from these secreted cytokines because neutralization of IL-8 in coculture media led to decreased cell adhesion

---

FIGURE 6 FOS is a downstream target repressed by BACH2 expression in pre-B leukemic cells. A, Correlation analyses of *BACH2* and *FOS* expression based on microarray data in B cell acute lymphoblastic leukemia (B-ALL) at new diagnosis (ND) (n = 238). *R* value and *P* value are indicated. B, *BACH2* and *FOS* mRNA levels in pediatric ALL (p-ALL) samples including B-ALL (n = 10), T cell ALL (T-ALL) and B/T cell mixed-phenotype acute leukemia (B/T MPAL) (n = 2) with two immune thrombocytopenic purpura (ITP) samples as negative controls. The fold change in expression compared with the *BACH2* levels of one B-ALL patient is indicated. Data are shown as the mean ± SEM. C, Immunoblots of FOS in different subtypes of p-ALL with one ITP sample as a negative control. GAPDH was used as a loading control. D, Three putative MARE binding sites within *FOS* proximal promoter (MARE1), 5′ untranslated region (5′ UTR, MARE2), and Exon 1 (MARE3) along with truncated promoter constructs are indicated (left). 293T cells were transfected with truncated promoter plasmids, BACH2 expression plasmids, or control plasmids (pcDNA3.1). An empty pGL3-basic plasmid was used as a negative control. The *Renilla* luciferase reporter pRL-SV40 was used as an internal control for normalization. Luciferase activity was measured 48 h after transfection. Data are presented as the relative luciferase activity compared with the cells with pcDNA3.1 expression. Data are shown as the mean ± SD from three independent experiments. E, Peak analysis by an IGV software following CUT&Tag sequencing is indicated, with orange reads representing antibodies against control IgG and blue reads representing antibodies against BACH2. GRCh38 genome was used as a human reference genome. Peaks corresponding to MARE1, MARE2, and MARE3 are indicated (red arrows). F, DNA fragments (a-e) in Nalm-6 cells amplified by PCR following CUT&Tag assays are indicated (upper), and the relative intensity of each band is shown from two independent validations (lower). NS, not significant; *P < .05; **P < .01; ***P < .001. BM, bone marrow

(A) FOS expression values vs BACH2 expression values, B-ALL (n=238), R= −0.3630, p< 0.0001

(B) BACH2 / FOS, Relative mRNA levels (fold), B-ALL (n=10), T-ALL and B/T MPAL (n=2), ITP (n=2)

(C) Pediatric ALL BM samples: Others (Pt #2), ETV6-RUNX1 (Pt #3), BCR-ABL1 (Pt #9), T-ALL (Pt #7), ITP (ITP #1); FOS: 1.54, 0.76, 1.55, 0.21, 0.08; GAPDH

(D) proximal promoter and 5' UTR; −1050, −212, +32, +181, Exon 1 (+1 ~ +296), MARE1, TSS, MARE2, MARE3, hFOS, ATG (+156); LUC → pGL3-basic; pGL3-MARE1: −212 → CTGAGACAGGA ← −202; pGL3-MARE2: +32 → AAGACTGAGCCG ← +43; pGL3-MARE3: +181 → ACTACGAGGCGT ← +192; 293T, pcDNA3.1 / pcDNA3.1-BACH2, Relative luciferase expression

(E) 16 kb; IgG; BACH2; MARE1, MARE2, MARE3; FOS; Nalm-6

(F) Nalm-6; a b c d e; BACH2; IgG; BACH2/IgG (fold); IgG / BACH2

to BMSCs (Figure 5D), whereas GM-CSF– or IL-6–neutralizing antibodies increased Ara-C–derived cytotoxicity (Figure 5E). These results indicated that stromal microenvironmental alterations have many tumor-promoting effects that not only enhance cell adhesion but also protect leukemic cells from Ara-C–derived cytotoxicity in ALL.

3.6 | Proto-oncoprotein FOS is a novel downstream target repressed by BACH2 in pre-B leukemic cells

BACH2 is a basic region leucine zipper (bZIP) protein that forms heterodimers with the small Maf proteins.[36] The BACH2-Maf heterodimers repress transcription by binding to DNA sequences termed Maf recognition elements [MARE, 5′-TGCTGA(G/C) TCAGCA-3′).[10,36] Interestingly, MARE includes a core TPA response element [TRE, 5′-TGA(G/C)TCA-3′] that can be bound by activator protein 1 (AP-1), a dimeric transcriptional activator formed by JUN and FOS.[6] Therefore, BACH2 regulates gene expression by competing with the AP-1 complex.[6] Despite well-established oncogenic functions of AP-1 signaling,[37-40] each component of the AP-1 complex plays independent roles. JUN is involved in tumorigenesis by regulating malignant transformation, apoptosis, angiogenesis, and DNA methylation,[41-45] whereas FOS, in addition to a similar role to JUN,[46-48] plays an extra role in regulating bone cell differentiation and osteoimmunology.[49] Mice lacking Fos develop severe osteopetrosis with deficiencies in bone remodeling[50] and exhibit altered B cell differentiation due to an impaired BM microenvironment.[51] In BCR-ABL1–induced leukemia, FOS was recently identified as one of critical mediators for leukemogenesis and imatinib resistance.[52] Given a similar effect of BACH2 and FOS on BM microenvironmental regulation, we hypothesized that FOS might correlate with BACH2 in p-ALL.

To test this hypothesis, we started with the correlation analysis of *BACH2* and *FOS* expressions using published microarray data (GSE28497), which showed a significant inverse correlation between them in B-ALL at ND (Figure 6A); however, we did not find an inverse but observed a positive correlation between *BACH2* and *FOS* in T-ALL (Figure S5A), implying a totally different regulatory network of BACH2 in T cells.

Next, we detected the mRNA levels of *BACH2* and *FOS* in clinical p-ALL samples, and the same inverse correlation was found in B-ALL at ND, except T-ALL and B/T MPAL cases (Figure 6B and Figure S5B). Further immunoblots showed differential expression of FOS protein among different subtypes (Figure 6C), coinciding with the corresponding BACH2 levels in the B-ALL group (Figure 2E). In leukemic cell lines, *FOS* levels were also increased after BACH2 silencing while reduced upon BACH2 overexpression (Figure S5C). These results indicated that BACH2 is very likely a potential suppressing regulator of FOS in leukemic cells.

We next wondered whether the *FOS* gene is a transcriptional target repressed by BACH2 protein. Based on sequence alignment methods, we identified three potential MARE binding sites of the *FOS* gene within ± 1000 bp, which are located at the proximal promoter (MARE1, −212/−202), 5′ untranslated region (MARE2, +32/+43), and Exon 1 (MARE3, +181/+192), respectively (Figure 6D). Truncated luciferase reporters containing different numbers of putative MAREs were constructed respectively. The luciferase activity of pGL3-MARE3 was significantly decreased in 293T cells when cotransfected with BACH2 expression plasmids compared with the controls (Figure 6D). Further sequencing using CUT&Tag, a next-generation technique to investigate interactions between proteins and DNA instead of a chromatin immunoprecipitation (ChIP) assay, confirmed BACH2-*FOS* interaction in Nalm-6 cells (Figure 6E). Indeed, two most enriched regions (fragments b and c) of the *FOS* gene containing BACH2-binding sites were further validated by PCR amplification (Figure 6F and Figure S6). These findings support that BACH2 suppresses *FOS* transcription by binding to MARE sites around the transcription start site (TSS) of the *FOS* gene.

## 3.7 | Blocking FOS by small molecule inhibitors sensitizes leukemic cells to Ara-C in xenografts

Given that the *FOS* gene is a downstream target repressed by BACH2, we then reasoned that FOS might be functionally involved in BACH2-induced BM microenvironmental alterations and Ara-C resistance. We firstly tested the effects of two chemical compounds targeting FOS, nordihydroguaiaretic acid (NDGA) and curcumin,[52] on microenvironmental secretion of cytokines in a coculture setting of BACH2[KD] Nalm-6 and HS-5 cells. Both NDGA and curcumin were effective in suppressing the secretion of GM-CSF, IL-6, and IL-8 in coculture media (Figure S7A). In particular, blocking FOS with NDGA or curcumin obviously sensitized Ara-C–resistant BACH2[KD] Nalm-6 cells (Figure S7B) or primary cells (Figure 7A) to Ara-C in coculture media, suggesting that FOS is a very important mediator responsible for BACH2-induced microenvironmental changes and Ara-C resistance. The synergistic cytotoxic effects of Ara-C and NDGA/curcumin were further analyzed by combination index (CI) plots, which were all less than 1, indicating dramatic synergistic responses (Figure S8), in which more synergistic efficacy of Ara-C and NDGA was observed than the combination of Ara-C with curcumin.

FIGURE 7 Chemical inhibition of FOS sensitizes leukemic cells to Ara-C in primary samples and xenografts. A, Primary cells were cultured in complete RPMI1640 media (normal media, upper) or coculture media (lower) upon treatment of Ara-C at a low dosage of 20 nmol/L or a high dosage of 200 nmol/L for 48 h in the presence of nordihydroguaiaretic acid (NDGA), curcumin, or both. DMSO was used as a negative control. Cell viability was determined using MTT assays. Data are normalized to nontreated control cells and shown as the mean ± SD from three independent experiments. *P < .05; **P < .01; ***P < .001 (vs Ara-C + DMSO group). B, Experimental design for testing the efficacy of small molecule inhibitors of FOS (NDGA and curcumin) in vivo. C, Spleens (SPs) were isolated and photographed against a ruler (left). The sizes of SPs in each treatment group were measured (right). Data are shown as the mean ± SEM. NS, not significant; *P < .05; **P < .01 (vs Ara-C group). N, NDGA; C, curcumin. hCD19^{+} cells were isolated from SP (D) and bone marrow (BM) (E) using anti-hCD19-MicroBeads, and the % of hCD19^{+} cells in each organ was calculated. Data are shown as the mean ± SEM. NS, not significant; *P < .05; **P < .01 (vs Ara-C group). F, Survival curve of xenograft mice treated with PBS (black), Ara-C alone (green), or Ara-C in combination with NDGA (Ara-C+N, blue), curcumin (Ara-C+C, red), or both (Ara-C+both, purple)
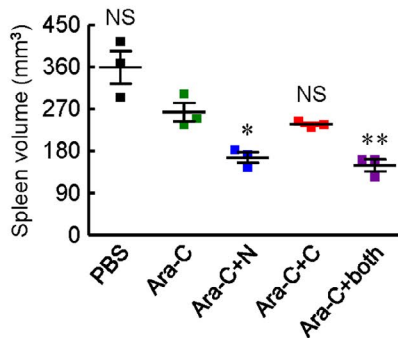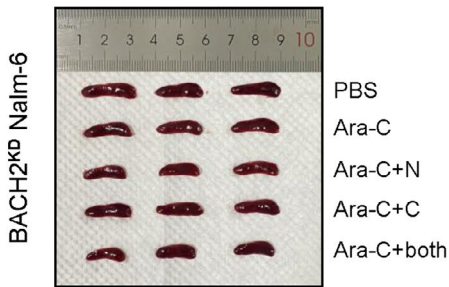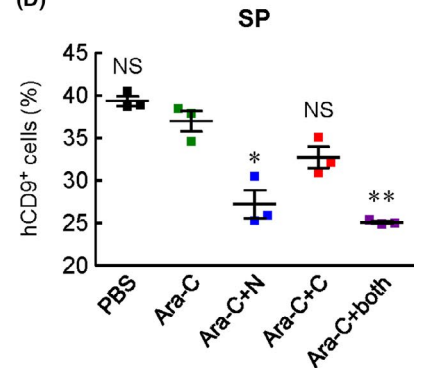
(A)

Normal media

☐ Control ◼ Ara-C+DMSO ◼ Ara-C+NDGA ◼ Ara-C+curcumin ◼ Ara-C+both
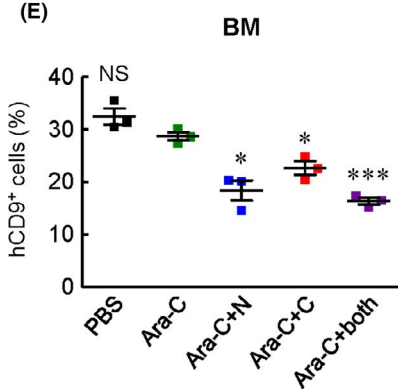

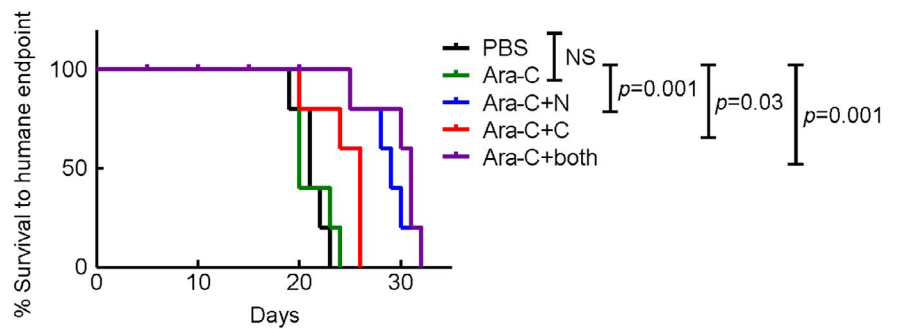Coculture media
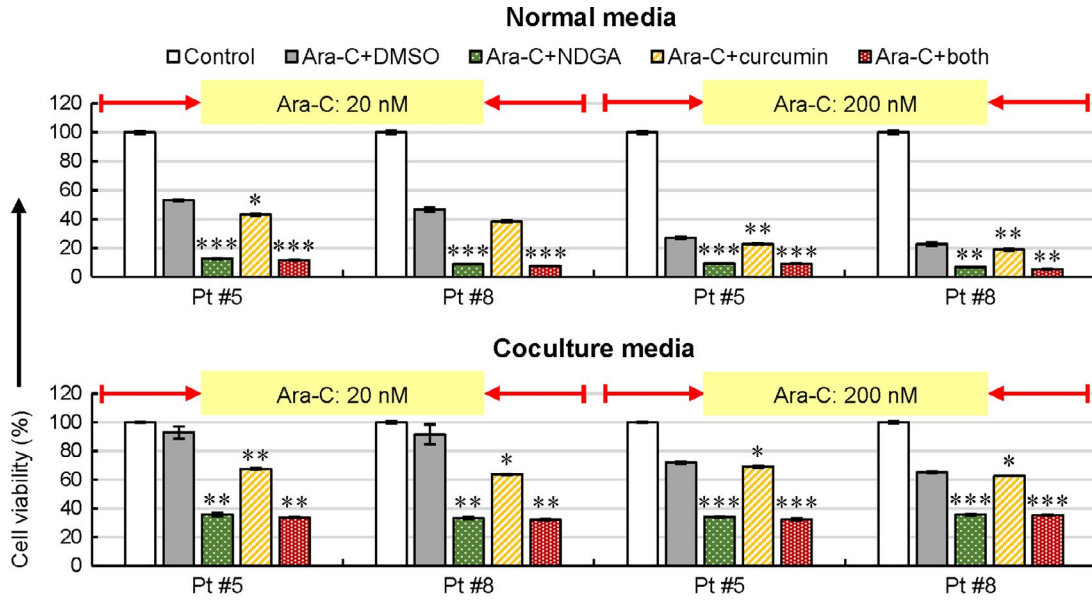
(B)
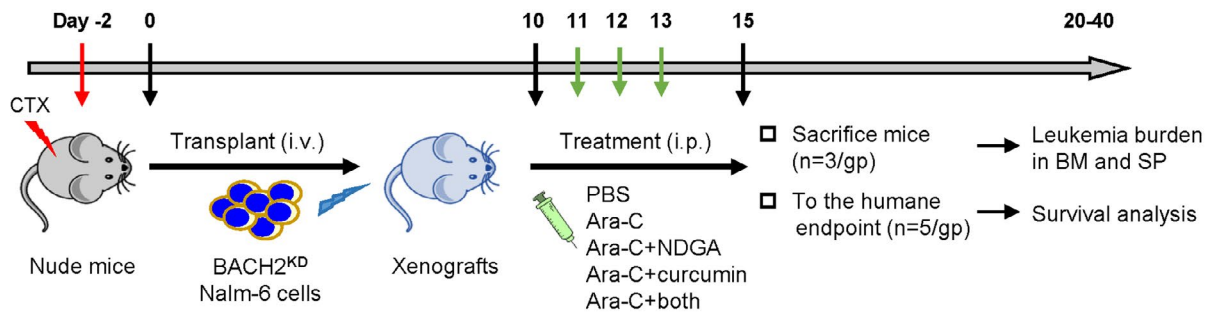
(C)

(D)

(E)

(F)

Next, we tested whether blocking FOS function is also effective in leukemia xenograft models. Ten days after intravenous transplantation of Ara-C–resistant BACH2[KD] Nalm-6 cells, mice were treated with Ara-C alone or in combination with NDGA (Ara-C+N), curcumin (Ara-C+C), or both (Ara-C+both) for 3 days and euthanized 2 days later (Figure 7B). Mice treated with Ara-C+N or Ara-C+both significantly reduced splenomegaly after one course of treatment (Figure 7C). Combined treatment with Ara-C+N or Ara-C+both also led to a more effective inhibition of leukemia burden in SP and BM compared with the single-agent Ara-C group (Figure 7D-E). In a separate cohort, mice treated with Ara-C+N or Ara-C+both showed improved survival compared with other groups (Figure 7F), suggesting that the combined treatment is effective to prolong survival of tumor-bearing animals.

4 | DISCUSSION

Despite incremental success in the treatment of p-ALL, much still remains to be achieved: Not all patients receive optimal therapy, and cure rates remain modest or even poorer in high-risk groups such as *BCR-ABL1*^{+} B-ALL, T-ALL, and MPAL cases. Tremendous advances have been witnessed in the understanding of the genetic basis of p-ALL by the application of next-generation sequencing technologies,[14,53] however, we are still far from fully deciphering the molecular pathogenesis of p-ALL and the mechanisms underlying RE and treatment failure.

In the current study, we found downregulation of BACH2 in children with unfavorable *BCR-ABL1* fusion gene compared with other subtypes in B-ALL. This finding is supported by a study demonstrating that BACH2 is a direct transcriptional target repressed by BCR-ABL1 oncoprotein via suppression of PAX5 expression in chronic myeloid leukemia cells.[12] In contrast, we are surprised to observe much higher levels of *BACH2* in *TCF3-PBX1*^{+} subtype at ND than a well-recognized favorable *ETV6-RUNX1*^{+} subtype,[23] as ALL with *TCF3-PBX1* was once associated with a poor prognosis. With contemporary MRD-stratified therapy, *TCF3-PBX1*^{+} subtype is now classified as a low-to-intermediate risk genotype.[23,54] Children with *TCF3-PBX1* treated with Berlin-Frankfurt-Münster (BFM) or Chinese Children's Leukemia Group (CCLG)-ALL protocols get even better event-free survival rates than those without *TCF3-PBX1*.[55-57] The improved outcome of *TCF3-PBX1*^{+} subtype in p-ALL might be attributed to higher levels of BACH2, which facilitates efficient chemotherapies by sensitizing leukemic cells to agents. Indeed, we found ectopic expression of BACH2 in leukemic cells shows higher sensitivity to Ara-C, whereas downregulation of BACH2 confers Ara-C resistance properties to leukemic cells.

In addition, we discovered extremely low levels of BACH2 in T-ALL and B/T MPAL cases. Unlike B-ALL, the genetic basis of T-ALL predisposition remains poorly understood, and no consensus genetic classification with prognostic or therapeutic implications has been reached for T-ALL; therefore, the precision medicine approaches for T-ALL are lagging far behind in children.[23] Likewise, B/T

MPAL, a particularly rare and understudied subtype of ALL, defines a high-risk subgroup with an inferior outcome, no matter what classification is used.[24,58] Although early MRD response is clinically useful in tailoring treatment, MRD detection is currently limited by its technical complexity. In this regard, identification and molecular characterization of new factors, such as BACH2, can provide new insights into the pathogenesis of p-ALL, yet offering an alternative molecular marker during the early induction phase and a new opportunity for the development of therapeutic targets.

Despite our findings of BACH2 biological features in clinical samples and leukemic cells, it is still unclear whether BACH2 is an original cause or just a mediator of other causative factors and cellular perturbation in p-ALL. Here, we found silencing BACH2 enhances adhesion of leukemic cells to BMSCs by upregulating GM-CSF, IL-6, and IL-8, which further leads to Ara-C resistance within the surrounding stroma. These aberrant cytokines may not be the only abnormal factors in the BM microenvironment for ALL. Rather, this finding provides a proof of concept that leukemic cells in the BM have capacities for interacting with BMSCs and activating aberrant signaling pathways, which may uniquely or collectively alter the BM microenvironment, thus contributing to the survival and progression of ALL.

In fact, it has proved difficult to target tumor suppressors, such as p53, for cancer treatment because the development of reactivator drugs to recover the wild-type activity is much harder than designing drugs targeting cancer driver genes.[59] The same might be true for BACH2. Therefore, it requires new thinking or a different approach to target BACH2; for example, to target the downstream factors or cofactors of BACH2 instead. We found an inverse correlation between BACH2 and FOS in children with B-ALL. Of particular interest to us, FOS, as well as being a transcriptional activator competing with BACH2, itself is also a downstream target repressed by BACH2. Our finding of BACH2-FOS signaling axis partially explains the microenvironmental alterations and Ara-C resistance in BM, adding a new layer in the understanding of BACH2-mediated anticancer functions in p-ALL. Inspiringly, blocking FOS by NDGA or curcumin, either alone or in combination, remarkably synergized with Ara-C to battle against Ara-C–resistant BACH2[KD] cells, especially in the resistant coculture setting. Our experiments with BACH2[KD] leukemia xenografts treated with FOS inhibitors further provided strong evidence for this. These findings suggest a novel therapeutic strategy to efficiently overcome Ara-C resistance in p-ALL. Although no other chemo-agents but Ara-C were investigated in this study, the discovery of BACH2-mediated Ara-C resistance may shed light on other oxidative stress agents, such as etoposide,[10] a topic that needs further investigation.

In conclusion, aberrant BACH2 levels in p-ALL may serve as a novel indicator for risk stratification and early treatment responses. Our discovery of the inverse correlation between BACH2 and FOS provides the proof of p-ALL progression and Ara-C resistance in surrounding BM stromal microenvironment. Future efforts to fully depict the regulatory network of BACH2 in p-ALL will uncover more significant clues on the treatment of p-ALL and identify additional

interactive partners of BACH2, if any, that are vital for the pathogenesis and chemoresistance of p-ALL.

DISCLOSURE

The authors declare no conflict of interest.

ORCID

Han Zhang https://orcid.org/0000-0002-2684-512X

REFERENCES

1. Muto A, Tashiro S, Nakajima O, et al. The transcriptional programme of antibody class switching involves the repressor Bach2. *Nature*. 2004;429(6991):566-571.
2. Huang C, Geng H, Boss I, Wang L, Melnick A. Cooperative transcriptional repression by BCL6 and BACH2 in germinal center B-cell differentiation. *Blood*. 2014;123(7):1012-1020.
3. Itoh-Nakadai A, Matsumoto M, Kato H, et al. A Bach2-Cebp gene regulatory network for the commitment of multipotent hematopoietic progenitors. *Cell Rep*. 2017;18(10):2401-2414.
4. Itoh-Nakadai A, Hikota R, Muto A, et al. The transcription repressors Bach2 and Bach1 promote B cell development by repressing the myeloid program. *Nat Immunol*. 2014;15(12):1171-1180.
5. Swaminathan S, Huang C, Geng H, et al. BACH2 mediates negative selection and p53-dependent tumor suppression at the pre-B cell receptor checkpoint. *Nat Med*. 2013;19(8):1014-1022.
6. Igarashi K, Kurosaki T, Roychoudhuri R. BACH transcription factors in innate and adaptive immunity. *Nat Rev Immunol*. 2017;17(7):437-450.
7. Roychoudhuri R, Hirahara K, Mousavi K, et al. BACH2 represses effector programs to stabilize T(reg)-mediated immune homeostasis. *Nature*. 2013;498(7455):506-510.
8. Tsukumo S, Unno M, Muto A, et al. Bach2 maintains T cells in a naive state by suppressing effector memory-related genes. *Proc Natl Acad Sci USA*. 2013;110(26):10735-10740.
9. Sakane-Ishikawa E, Nakatsuka S, Tomita Y, et al. Prognostic significance of BACH2 expression in diffuse large B-cell lymphoma: a study of the Osaka Lymphoma Study Group. *J Clin Oncol*. 2005;23(31):8012-8017.
10. Kamio T, Toki T, Kanezaki R, et al. B-cell-specific transcription factor BACH2 modifies the cytotoxic effects of anticancer drugs. *Blood*. 2003;102(9):3317-3322.
11. Zhang H, Chen Z, Miranda RN, Medeiros LJ, McCarty N. Bifurcated BACH2 control coordinates mantle cell lymphoma survival and dispersal during hypoxia. *Blood*. 2017;130(6):763-776.
12. Casolari DA, Makri M, Yoshida C, Muto A, Igarashi K, Melo JV. Transcriptional suppression of BACH2 by the Bcr-Abl oncoprotein is mediated by PAX5. *Leukemia*. 2013;27(2):409-415.
13. Sasaki S, Ito E, Toki T, et al. Cloning and expression of human B cell-specific transcription factor BACH2 mapped to chromosome 6q15. *Oncogene*. 2000;19(33):3739-3749.
14. Pui CH, Nichols KE, Yang JJ. Somatic and germline genomics in paediatric acute lymphoblastic leukaemia. *Nat Rev Clin Oncol*. 2019;16(4):227-240.

15. Pui CH, Yang JJ, Hunger SP, et al. Childhood acute lymphoblastic leukemia: progress through collaboration. *J Clin Oncol*. 2015;33(27):2938-2948.
16. Hunger SP, Mullighan CG. Acute lymphoblastic leukemia in children. *N Engl J Med*. 2015;373(16):1541-1552.
17. Coustan-Smith E, Song G, Clark C, et al. New markers for minimal residual disease detection in acute lymphoblastic leukemia. *Blood*. 2011;117(23):6267-6276.
18. Bhojwani D, Kang H, Moskowitz NP, et al. Biologic pathways associated with relapse in childhood acute lymphoblastic leukemia: a Children's Oncology Group study. *Blood*. 2006;108(2):711-717.
19. Holleman A, Cheok MH, den Boer ML, et al. Gene-expression patterns in drug-resistant acute lymphoblastic leukemia cells and response to treatment. *N Engl J Med*. 2004;351(6):533-542.
20. Garnett MJ, Edelman EJ, Heidorn SJ, et al. Systematic identification of genomic markers of drug sensitivity in cancer cells. *Nature*. 2012;483(7391):570-575.
21. Zhang H, Chen Z, Neelapu SS, Romaguera J, McCarty N. Hedgehog inhibitors selectively target cell migration and adhesion of mantle cell lymphoma in bone marrow microenvironment. *Oncotarget*. 2016;7(12):14350-14365.
22. Robinson JT, Thorvaldsdottir H, Winckler W, et al. Integrative genomics viewer. *Nat Biotechnol*. 2011;29(1):24-26.
23. Teachey DT, Pui CH. Comparative features and outcomes between paediatric T-cell and B-cell acute lymphoblastic leukaemia. *Lancet Oncol*. 2019;20(3):e142-e154.
24. Wolach O, Stone RM. How I treat mixed-phenotype acute leukemia. *Blood*. 2015;125(16):2477-2485.
25. Kanno S, Hiura T, Ohtake T, et al. Characterization of resistance to cytosine arabinoside (Ara-C) in NALM-6 human B leukemia cells. *Clin Chim Acta*. 2007;377(1–2):144-149.
26. Kanno S, Hiura T, Shouji A, Osanai Y, Ujibe M, Ishikawa M. Resistance to Ara-C up-regulates the activation of NF-kappaB, telomerase activity and Fas expression in NALM-6 cells. *Biol Pharm Bull*. 2007;30(11):2069-2074.
27. Muto A, Tashiro S, Tsuchiya H, et al. Activation of Maf/AP-1 repressor Bach2 by oxidative stress promotes apoptosis and its interaction with promyelocytic leukemia nuclear bodies. *J Biol Chem*. 2002;277(23):20724-20733.
28. Jacamo R, Chen Y, Wang Z, et al. Reciprocal leukemia-stroma VCAM-1/VLA-4-dependent activation of NF-kappaB mediates chemoresistance. *Blood*. 2014;123(17):2691-2702.
29. Bendall LJ, Kortlepel K, Gottlieb DJ. Human acute myeloid leukemia cells bind to bone marrow stroma via a combination of beta-1 and beta-2 integrin mechanisms. *Blood*. 1993;82(10):3125-3132.
30. Matsunaga T, Takemoto N, Sato T, et al. Interaction between leukemic-cell VLA-4 and stromal fibronectin is a decisive factor for minimal residual disease of acute myelogenous leukemia. *Nat Med*. 2003;9(9):1158-1165.
31. Zeng Z, Samudio IJ, Munsell M, et al. Inhibition of CXCR4 with the novel RCP168 peptide overcomes stroma-mediated chemoresistance in chronic and acute leukemias. *Mol Cancer Ther*. 2006;5(12):3113-3121.
32. Kim JA, Shim JS, Lee GY, et al. Microenvironmental remodeling as a parameter and prognostic factor of heterogeneous leukemogenesis in acute myelogenous leukemia. *Cancer Res*. 2015;75(11):2222-2231.
33. Roecklein BA, Torok-Storb B. Functionally distinct human marrow stromal cell lines immortalized by transduction with the human papilloma virus E6/E7 genes. *Blood*. 1995;85(4):997-1005.
34. Yin T, Li L. The stem cell niches in bone. *J Clin Invest*. 2006;116(5):1195-1201.
35. Colmone A, Amorim M, Pontier AL, Wang S, Jablonski E, Sipkins DA. Leukemic cells create bone marrow niches that disrupt the behavior of normal hematopoietic progenitor cells. *Science*. 2008;322(5909):1861-1865.

36. Oyake T, Itoh K, Motohashi H, et al. Bach proteins belong to a novel family of BTB-basic leucine zipper transcription factors that interact with MafK and regulate transcription through the NF-E2 site. *Mol Cell Biol*. 1996;16(11):6083-6095.

37. Young MR, Li JJ, Rincon M, et al. Transgenic mice demonstrate AP-1 (activator protein-1) transactivation is required for tumor promotion. *Proc Natl Acad Sci USA*. 1999;96(17):9827-9832.

38. Jochum W, Passegue E, Wagner EF. AP-1 in mouse development and tumorigenesis. *Oncogene*. 2001;20(19):2401-2412.

39. Liu Y, Ludes-Meyers J, Zhang Y, et al. Inhibition of AP-1 transcription factor causes blockade of multiple signal transduction pathways and inhibits breast cancer growth. *Oncogene*. 2002;21(50):7680-7689.

40. Motiwala T, Zanesi N, Datta J, et al. AP-1 elements and TCL1 protein regulate expression of the gene encoding protein tyrosine phosphatase PTPROt in leukemia. *Blood*. 2011;118(23):6132-6140.

41. Bakiri L, Lallemand D, Bossy-Wetzel E, Yaniv M. Cell cycle-dependent variations in c-Jun and JunB phosphorylation: a role in the control of cyclin D1 expression. *EMBO J*. 2000;19(9):2056-2068.

42. Eferl R, Ricci R, Kenner L, et al. Liver tumor development. c-Jun antagonizes the proapoptotic activity of p53. *Cell*. 2003;112(2):181-192.

43. Vleugel MM, Greijer AE, Bos R, van der Wall E, van Diest PJ. c-Jun activation is associated with proliferation and angiogenesis in invasive breast cancer. *Hum Pathol*. 2006;37(6):668-674.

44. Mariani O, Brennetot C, Coindre JM, et al. JUN oncogene amplification and overexpression block adipocytic differentiation in highly aggressive sarcomas. *Cancer Cell*. 2007;11(4):361-374.

45. Kollmann K, Heller G, Ott RG, et al. c-JUN promotes BCR-ABL-induced lymphoid leukemia by inhibiting methylation of the 5' region of Cdk6. *Blood*. 2011;117(15):4065-4075.

46. Wang ZQ, Grigoriadis AE, Mohle-Steinlein U, Wagner EF. A novel target cell for c-fos-induced oncogenesis: development of chondrogenic tumours in embryonic stem cell chimeras. *EMBO J*. 1991;10(9):2437-2450.

47. Grigoriadis AE, Schellander K, Wang ZQ, Wagner EF. Osteoblasts are target cells for transformation in c-fos transgenic mice. *J Cell Biol*. 1993;122(3):685-701.

48. Milde-Langosch K. The Fos family of transcription factors and their role in tumourigenesis. *Eur J Cancer*. 2005;41(16):2449-2461.

49. Wagner EF, Eferl R. Fos/AP-1 proteins in bone and the immune system. *Immunol Rev*. 2005;208:126-140.

50. Wang ZQ, Ovitt C, Grigoriadis AE, Mohle-Steinlein U, Ruther U, Wagner EF. Bone and haematopoietic defects in mice lacking c-fos. *Nature*. 1992;360(6406):741-745.

51. Okada S, Wang ZQ, Grigoriadis AE, Wagner EF, von Ruden T. Mice lacking c-fos have normal hematopoietic stem cells but exhibit altered B-cell differentiation due to an impaired bone marrow environment. *Mol Cell Biol*. 1994;14(1):382-390.

52. Kesarwani M, Kincaid Z, Gomaa A, et al. Targeting c-FOS and DUSP1 abrogates intrinsic resistance to tyrosine-kinase inhibitor therapy in BCR-ABL-induced leukemia. *Nat Med*. 2017;23(4):472-482.

53. Roberts KG, Mullighan CG. Genomics in acute lymphoblastic leukaemia: insights and treatment implications. *Nat Rev Clin Oncol*. 2015;12(6):344-357.

54. Iacobucci I, Mullighan CG. Genetic basis of acute lymphoblastic leukemia. *J Clin Oncol*. 2017;35(9):975-983.

55. Kager L, Lion T, Attarbaschi A, et al. Incidence and outcome of TCF3-PBX1-positive acute lymphoblastic leukemia in Austrian children. *Haematologica*. 2007;92(11):1561-1564.

56. Felice MS, Gallego MS, Alonso CN, et al. Prognostic impact of t(1;19)/ TCF3-PBX1 in childhood acute lymphoblastic leukemia in the context of Berlin-Frankfurt-Munster-based protocols. *Leuk Lymphoma*. 2011;52(7):1215-1221.

57. Hu Y, He H, Lu J, et al. E2A-PBX1 exhibited a promising prognosis in pediatric acute lymphoblastic leukemia treated with the CCLG-ALL2008 protocol. *Onco Targets Ther*. 2016;9:7219-7225.

58. Mi X, Griffin G, Lee W, et al. Genomic and clinical characterization of B/T mixed phenotype acute leukemia reveals recurrent features and T-ALL like mutations. *Am J Hematol*. 2018;93(11):1358-1367.

59. Duffy MJ, Synnott NC, O'Grady S, Crown J. Targeting p53 for the treatment of cancer. *Semin Cancer Biol*. 2020;S1044-579X(20):30160-30167.

SUPPORTING INFORMATION

Additional supporting information may be found online in the Supporting Information section.